

---

---

CATALYSIS

---

---

## A Study of a Catalyst Based on Oxides of Base Transition Metals for Decomposition of Ozone and Oxidation of Toxic Organic Compounds

S. N. Tkachenko, E. Z. Golozman, V. V. Lunin, I. V. Kozlova, G. V. Egorova,  
E. A. Boevskaya, I. S. Tkachenko, A. I. Nechugovskii, and M. P. Yaroshenko<sup>1</sup>

*Lomonosov State University, Moscow, Russia*

*Novomoskovsk Institute of Nitrogen Industry, Open Joint-Stock Company, Novomoskovsk,  
Tula oblast, Russia*

*TIMIS Research-and-Promotion Firm, Limited Liability Company, Moscow, Russia*

Received August 29, 2006; in final form, March 2007

**Abstract**—Cement-containing GTT catalysts based on manganese, copper, and nickel oxides were developed and introduced into practice in processes employing ozone technologies and in oxidation of toxic organic compounds. Physicochemical methods were used to study the process of catalyst formation and the influence exerted by various brands of manganese salts and by preparation conditions and, in particular, calcination temperatures and grain molding technique on the characteristics of the catalytic systems obtained. Several commercial batches of GTT catalysts were manufactured.

**DOI:** 10.1134/S1070427207080174

At present, one of the most efficient and ecologically safe ways to purify drinking water, wastewater, and water in swimming pools is ozonation. The use of ozone is due to its oxidizing and bactericidal properties; however, the acrid smell and toxicity of ozone ( $MPC = 3.3 \mu\text{g m}^{-3}$ ) makes topical the problem of destruction of residual ozone [1]. Photochemical, thermal, and catalytic methods of ozone decomposition are possible. The optimal in economical efficiency and simplicity of technological apparatus is the catalytic decomposition of ozone [2].

The industrially employed catalyst for ozone decomposition, hopcalite, is composed of 60% manganese oxide, 25% copper oxide, and 15% binder (bentonite clay). It has an important disadvantage, poor mechanical strength, to the point of grain disintegration under the action of moisture drops [3]. The known catalysts [4], distinguished by stability and operation

efficiency under humid conditions, contain noble metals and, in particular, silver and are rather expensive.

Catalysts composed of oxides of nonprecious transition metals and exhibiting stable operation under various conditions have been created by developing cement-containing catalysts of GTT and GT brands, based on manganese, copper, and nickel oxides [5–9]. The activity of these catalysts in a dry flow is close to that of hopcalite and exceeds it by a factor of 1.5–2 in operation in a humid flow. These catalytic systems have high mechanical strength and water resistance, and their grains preserve shape when brought in contact with water. In a dry gas flow, the catalysts work at room temperature. In a humid flow, the working temperature range is 20–120°C. In case of a decrease in activity in a corrosive humid medium, the catalysts can be regenerated at 250–300°C in 2–3 h.

Tests demonstrated that GTT is efficient not only in ozone decomposition, but also in oxidation of carbon monoxide, methane, benzene, styrene, isopropylbenzene, butyl acetate, and other compounds. The GTT catalyst possesses the necessary developed surface, thermal stability, and resistance to coking in

---

<sup>1</sup> N.I. Murashov, Zh.V. Myasnikova, S.G. Dormidontova, and L.D. Kvasova took part in catalyst preparation on laboratory, pilot, and industrial installations, and also in catalytic activity tests and determination of other characteristics of catalysts.

**Table 1.** Basic characteristics of the cement-containing GTT catalyst (for extrudates)

Parameter	Grains of dark brown to black color
Bulk density, kg dm <sup>-3</sup> , no more than	1.3
Mechanical strength, kg mm <sup>-1</sup> grain diameter, no less than:	
average	1.1
minimum	0.6
Porosity Π, %, no less than	40
Specific surface area $S_{sp}$ , m <sup>2</sup> g <sup>-1</sup> , no less than	100
Ozone decomposition factor* $\gamma$ in a gas flow, no less than:	
dry gas flow	$1.1 \times 10^{-4}$
humid gas flow	$0.55 \times 10^{-4}$

\* The quantity  $\gamma$ , the fraction of active, i.e., leading to decomposition, collisions of ozone molecules with the catalyst surface, is taken as a measure of the catalyst activity. The ozone decomposition factor is given by the Lunin–Popovich–Tkachenko formula [3]  $\gamma = 4w[\ln(c_0/c)]V_t S$ , where  $c_0$  and  $c$  are the ozone concentrations at the reactor inlet and outlet, respectively;  $w$ , volumetric gas flow rate;  $V_t$ , thermal motion velocity of molecules; and  $S$ , total external surface area of catalyst grains. The parameter  $\gamma$  is proportional to the effective rate constant of the heterogeneous decomposition of ozone.

oxidation of the chemical products mentioned above. The basic technical characteristics of GTT are listed in Table 1.

The technology of GTT fabrication has been implemented at the catalyst shop of NIAP. The catalyst is manufactured as compacted pellets  $d \times h = 6 \times 3$  ( $5 \times 3$ ) mm<sup>2</sup> and in the extruded form [extrudates with a diameter of 1.5 to 5 mm and length of 5 to 15 mm; pellets with  $d \times h = 5 \times 3$  ( $4 \times 3$ ) mm<sup>2</sup>].

The aim of this study was to examine, using a set of physicochemical techniques, the influence exerted by the preparation conditions and composition of the starting manganese-containing concentrate on the formation of the Mn–Cu–Ni–Al–Ca system and to determine the relationship between the phase composition of the catalyst and its catalytic activity in decomposition of ozone and oxidation of benzene.

## EXPERIMENTAL

The catalyst was fabricated by the method of hydrothermal synthesis (HTS) [10, 11], which includes mixing of the starting components in the presence of aqueous ammonia and granulation of the resulting paste, followed by keeping of the grains first in a humid-air medium and then in hot water in the stage of hydrothermal treatment (HTT). After that the catalyst is dried and calcined.

An X-ray diffraction analysis was carried out on a DRON-3 diffractometer (graphite monochromator, Cu $K_{\alpha}$  radiation, reflected beam). IR spectra were measured on a Specord 75-IR spectrophotometer, with

samples prepared by compaction with KBr. The specific surface area of catalyst samples was determined by the low-temperature adsorption technique (BET). The total porosity was found from the true and apparent densities. The apparent density was calculated by dividing the mass of a sample by its geometric volume. The true density was determined by pycnometry, from the volume of toluene absorbed by a sample. The error in determining the total porosity was  $\pm 5\%$ .

An X-ray phase analysis (XPA) demonstrated that the synthesis of the catalyst involves, in stages of molding, humid-air treatment, HTT, and drying, the reaction of interaction (heterogeneous ion exchange) between hydroxocarbonates of copper (CHC) and nickel (NHC) and calcium aluminates (talum: CA, CA<sub>2</sub>) to give hydroxo aluminates (HA) of nickel and copper and calcite CaCO<sub>3</sub> [12]. XPA does not reveal any interaction of the starting MnCO<sub>3</sub> with the above components, whereas IR spectroscopy indicates [13] that a certain amount of manganese ions can be incorporated into the lattice of gibbsite formed as a result of talum hydration.

The temperature at which a catalyst is calcined strongly affects its formation and catalytic activity. For GTT samples calcined at 100–800°C, the phase composition and catalytic activity in ozone decomposition and benzene oxidation were determined. At low calcination temperatures (100–200°C), the starting

<sup>2</sup> CA, CA<sub>2</sub> are designations used in cement chemistry: CA = CaO · Al<sub>2</sub>O<sub>3</sub> and CA<sub>2</sub> = CaO · 2Al<sub>2</sub>O<sub>3</sub>.

metal hydroxocarbonates and products of talum hydration and ion exchange are present. At higher temperatures, metal hydroxocarbonates decompose to the respective oxides. The starting manganese-containing component decomposes to oxides of various compositions. In the temperature range 300–350°C, a phase close in X-ray diffraction characteristics to  $\text{MnO}_2$  appears in the sample composition, the intensity of  $\text{Mn}_2\text{O}_3$ -related peaks increases, and the  $\text{Mn}_3\text{O}_4$  phase is weakly pronounced. At temperatures of 350–600°C, the content of  $\text{Mn}_3\text{O}_4$  increases, that of  $\text{Mn}_2\text{O}_3$  decreases, and  $\text{MnO}_2$  disappears. At 700–800°C the main manganese containing phase in  $\text{Mn}_3\text{O}_4$ .

Samples calcined in the temperature range 300–600°C show an ozone decomposition factor  $\gamma$  of no less than  $1.5 \times 10^{-4}$  (Fig. 1). Samples calcined at 400–600°C exhibited the highest activity in ozone decomposition [ $\gamma = (2.38\text{--}2.45) \times 10^{-4}$ ], and those calcined at 300–400°C, in benzene oxidation, with the temperature of benzene oxidation at 50% conversion equal to 230–240°C (Fig. 1). The decrease in the catalytic activity at calcination temperatures higher than 600°C is presumably due to recrystallization of the NiO and CuO phases. In accordance with this circumstance, the optimal temperature of catalyst calcination was chosen to be 350–400°C for ozone decomposition and 300–350°C for benzene oxidation.

The catalyst was prepared from different batches of a Mn-containing stock (Table 2) supplied under the brand Manganese hydroxocarbonate, which, according to XPA and IR spectral data, is anhydrous manganese carbonate, occasionally containing the  $\text{Mn}_2\text{O}_3$  phase. For example, the IR spectrum of sample no. 1 contains, together with absorption bands at 1420–1440, 870, and 730  $\text{cm}^{-1}$ , which characterize the carbonate anion in the composition of manganese carbonate, also strong absorption bands at 580–530  $\text{cm}^{-1}$ , related to the presence of an oxide phase (Fig. 2). According to XPA data, this is  $\text{Mn}_2\text{O}_3$ . The study revealed that no  $\text{MnCO}_3$  decomposition is observed up to 200°C; and at 300°C manganese oxides  $\text{Mn}_3\text{O}_4$  and  $\text{MnO}_2$  appear, together with  $\text{MnCO}_3$  and  $\text{Mn}_2\text{O}_3$ , in stock sample nos. 1 and 2 and only  $\text{Mn}_3\text{O}_4$  in sample no. 3. The  $\text{MnO}_2$  phase was not found in any of the stock samples at 400°C, and in the range 400–800°C  $\text{Mn}_2\text{O}_3$  is gradually converted to  $\text{Mn}_3\text{O}_4$ , which becomes the main manganese-containing phase at 800°C.

The above-mentioned brands of  $\text{MnCO}_3$  were used to prepare GTT catalyst samples under laboratory conditions. XPA data for GTT catalyst samples calcined at 300–500°C are listed in Table 3. The decomposition of  $\text{MnCO}_3$  in the catalyst occurs similarly to

**Table 2.** Phase composition of the manganese-containing stock at calcination temperatures of 200–800°C

T, °C	Phase composition		
	no. 1 $\text{MnCO}_3$ Sedema	no. 2 $\text{MnCO}_3$	no. 3 $\text{MnCO}_3$ (supply from Russia)
	supply from Belgium		
200	$\text{MnCO}_3, \text{Mn}_2\text{O}_3$	$\text{MnCO}_3$	$\text{MnCO}_3$
300	$\text{MnCO}_3, \text{Mn}_2\text{O}_3, \text{Mn}_3\text{O}_4, \text{MnO}_2$	$\text{MnCO}_3, \text{MnO}_2, \text{Mn}_3\text{O}_4, \text{Mn}_2\text{O}_3$	$\text{MnCO}_3, \text{Mn}_3\text{O}_4$
400	$\text{Mn}_2\text{O}_3, \text{Mn}_3\text{O}_4$	$\text{Mn}_2\text{O}_3, \text{Mn}_3\text{O}_4$	$\text{Mn}_3\text{O}_4, \text{MnCO}_3$
500	$\text{Mn}_2\text{O}_3, \text{Mn}_3\text{O}_4$	$\text{Mn}_2\text{O}_3, \text{Mn}_3\text{O}_4$	$\text{Mn}_2\text{O}_3, \text{Mn}_3\text{O}_4$
600	$\text{Mn}_2\text{O}_3, \text{Mn}_3\text{O}_4$	$\text{Mn}_2\text{O}_3, \text{Mn}_3\text{O}_4$	$\text{Mn}_2\text{O}_3, \text{Mn}_3\text{O}_4$
700	$\text{Mn}_2\text{O}_3, \text{Mn}_3\text{O}_4$	$\text{Mn}_2\text{O}_3, \text{Mn}_3\text{O}_4$	$\text{Mn}_2\text{O}_3, \text{Mn}_3\text{O}_4$
800	$\text{Mn}_3\text{O}_4$	$\text{Mn}_3\text{O}_4$	$\text{Mn}_3\text{O}_4$

that of the starting  $\text{MnCO}_3$ , although some distinctions are observed. At 300°C, the  $\text{MnO}_2$  phase appears in all the three samples. This phase is more pronounced in sample no. 2; further, at 350–500°C,

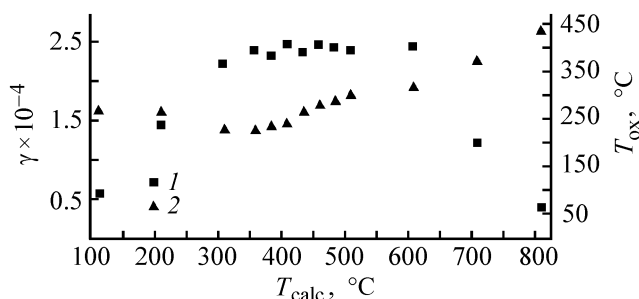


**Fig. 1.** Activity of the GTT catalyst in ozone decomposition and benzene oxidation vs. calcination temperature  $T_{\text{calc}}$ . ( $\gamma$ ) Ozone decomposition temperature and ( $T_{\text{ox}}$ ) temperature of 50% oxidation of benzene. (1) Ozone decomposition factor and (2) benzene oxidation temperature.

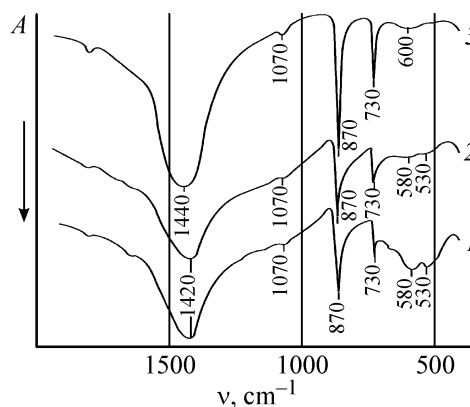


**Fig. 2.** IR spectra of uncalcined  $\text{MnCO}_3$  samples. (A) Absorption and ( $\nu$ ) wave number. Supply source: (1) Sedema, Belgium; (2) Belgium; and (3) Russia.

**Table 3.** Phase composition of GTT samples (based on various brands of MnCO<sub>3</sub>) calcined at 300–500°C

T, °C	Phase composition		
	no. 1 MnCO <sub>3</sub> Sedema	no. 2 MnCO <sub>3</sub>	no. 3 MnCO <sub>3</sub> (supply from Russia)
	supply from Belgium		
300	Mn <sub>2</sub> O <sub>3</sub> , MnO <sub>2</sub> , CA <sub>2</sub> , CaCO <sub>3</sub> , MnCO <sub>3</sub> , NiO, CuO	MnO <sub>2</sub> , CaCO <sub>3</sub> , CA <sub>2</sub> , MnCO <sub>3</sub> , NiO, CuO	MnCO <sub>3</sub> , MnO <sub>2</sub> , CaCO <sub>3</sub> , CA <sub>2</sub> , NiO, CuO
350	Mn <sub>2</sub> O <sub>3</sub> , Mn <sub>3</sub> O <sub>4</sub> , CaCO <sub>3</sub> , CA <sub>2</sub> , MnCO <sub>3</sub> , NiO, CuO	Mn <sub>3</sub> O <sub>4</sub> , CaCO <sub>3</sub> , Mn <sub>2</sub> O <sub>3</sub> , MnO <sub>2</sub> , CA <sub>2</sub> , MnCO <sub>3</sub> , NiO, CuO	MnO <sub>2</sub> , MnCO <sub>3</sub> , CaCO <sub>3</sub> , CA <sub>2</sub> , Mn <sub>2</sub> O <sub>3</sub> , NiO, CuO
400	Mn <sub>2</sub> O <sub>3</sub> , Mn <sub>3</sub> O <sub>4</sub> , CaCO <sub>3</sub> , CA <sub>2</sub>	Mn <sub>2</sub> O <sub>3</sub> , Mn <sub>3</sub> O <sub>4</sub> , CaCO <sub>3</sub> , MnO <sub>2</sub> , CA <sub>2</sub> , NiO, CuO	Mn <sub>3</sub> O <sub>4</sub> , CaCO <sub>3</sub> , Mn <sub>2</sub> O <sub>3</sub> , CA <sub>2</sub> , NiO, CuO
450	Mn <sub>2</sub> O <sub>3</sub> , CaCO <sub>3</sub> , Mn <sub>3</sub> O <sub>4</sub> , CA <sub>2</sub> , NiO, CuO	Mn <sub>2</sub> O <sub>3</sub> , Mn <sub>3</sub> O <sub>4</sub> , CaCO <sub>3</sub> , CA <sub>2</sub> , NiO, CuO	Mn <sub>3</sub> O <sub>4</sub> , Mn <sub>2</sub> O <sub>3</sub> , CaCO <sub>3</sub> , CA <sub>2</sub> , NiO, CuO
500	Mn <sub>2</sub> O <sub>3</sub> , Mn <sub>3</sub> O <sub>4</sub> , CA <sub>2</sub> , CaCO <sub>3</sub> , NiO, CuO	Mn <sub>2</sub> O <sub>3</sub> , Mn <sub>3</sub> O <sub>4</sub> , CaCO <sub>3</sub> , CA <sub>2</sub> , NiO, CuO	Mn <sub>2</sub> O <sub>3</sub> , Mn <sub>3</sub> O <sub>4</sub> , CaCO <sub>3</sub> , CA <sub>2</sub> , NiO, CuO

**Table 4.** Physicochemical characteristics and catalytic activity of GTT samples calcined at T = 400°C

GTT catalyst	Chemical composition: active components, %	$\gamma$	$T_{\text{benz.ox}}, ^\circ\text{C}$ , at 50% conversion	$S_{\text{sp}}, \text{m}^2 \text{g}^{-1}$	$\Pi, \%$
no. 1 MnCO <sub>3</sub> Sedema, supplied from Belgium	Mn <sub>3</sub> O <sub>4</sub> , 29.3, CuO, 19.6, NiO, 10.1; $\Sigma = 59$	$1.88 \times 10^{-4}$	250	100	70
no. 2 MnCO <sub>3</sub> , supplied from Belgium	Mn <sub>3</sub> O <sub>4</sub> , 28.6, CuO, 21.2, NiO, 10.3; $\Sigma = 60.1$	$1.85 \times 10^{-4}$	220	100	50
no. 3 MnCO <sub>3</sub> , supplied from Russia	Mn <sub>3</sub> O <sub>4</sub> , 29.6, CuO, 20.6, NiO, 10.9; $\Sigma = 61.1$	$1.85 \times 10^{-4}$	230	100	60

the content of this phase decreases and that of the oxides Mn<sub>2</sub>O<sub>3</sub> and Mn<sub>3</sub>O<sub>4</sub> increases, whereas in sample no. 3, mostly the content of the Mn<sub>3</sub>O<sub>4</sub> phase grows. Also, the degree of crystallinity of the copper oxide phase is higher at these temperature than that of nickel oxide. This is due to the fact that mostly the nickel hydroxoaluminate phase is formed in the preceding stages, and especially in the HTT stage, and this leads to formation of a dispersed phase of nickel oxide in calcination.

Table 4 lists physicochemical parameters of samples calcined at T = 400°C. The total amount of the active component in samples of a finished catalyst is 59 to 61%. The specific surface areas of the samples are virtually the same (~100 m<sup>2</sup> g<sup>-1</sup>). The highest porosity (~70%) is observed for GTT sample no. 1.

Activity tests of samples prepared from different stock batches demonstrated that, at close compositions and surface areas, all the samples exhibit high activity

in ozone decomposition,  $\gamma = (1.81\text{--}1.88) \times 10^{-4}$ . Consequently, presence of the Mn<sub>2</sub>O<sub>3</sub> phase in the starting manganese-containing component does not exert any significant influence on the GTT activity in ozone decomposition. However, a minor decrease in activity is observed in benzene oxidation: the difference in benzene oxidation temperature at 50% conversion is 20–30°C.

Extrudates were prepared on a pilot apparatus from MnCO<sub>3</sub> of Sedema brand, supplied from Belgium, and MnCO<sub>3</sub> from Russia. The ozone decomposition factor for batch no. 1 (extrudates 1.5 mm in diameter), synthesized from MnCO<sub>3</sub> containing an admixture of Mn<sub>2</sub>O<sub>3</sub> is 1.13–1.25 times lower than that for batch no. 2 (extrudates 1.5 mm in diameter), produced from MnCO<sub>3</sub> of domestic manufacture, in which the Mn<sub>2</sub>O<sub>3</sub> phase is either absent or present in a minor amount. GTT no. 1 is inferior to GTT no. 2 in specific surface area, porosity, and total amount of the active com-

**Table 5.** Physicochemical characteristics and catalytic activity of laboratory-pilot batches of extrudates and molded GTT pellets calcined at  $T = 415 \pm 15^\circ\text{C}$ 

GTT catalyst	XPA data for finished catalyst, $415 \pm 15^\circ\text{C}$	$\gamma$	$T_{\text{benz.ox}}, ^\circ\text{C}$ at 50% conversion	$S_{\text{sp}}, \text{m}^2 \text{g}^{-1}$	$\Pi, \%$	Chemical composition: active components, %
No. 1, extrudates, $d = 0.15$ cm, based on $\text{MnCO}_3$ Sedema, supplied from Belgium	$\text{Mn}_3\text{O}_4, \text{NiO}, \text{CaCO}_3, \text{CuO}, \text{Mn}_2\text{O}_3, \text{CA}_2$	$2.45 \times 10^{-4}$	240	110	40	$\text{Mn}_3\text{O}_4, 28.9, \text{CuO}, 18.5, \text{NiO}, 11.3; \Sigma = 58.6$
No. 2, extrudates, $d = 0.15$ cm, based on $\text{MnCO}_3$ , supplied from Russia	$\text{Mn}_3\text{O}_4, \text{CaO}_3, \text{NiO}, \text{CuO}, \text{CA}_2, \text{boehmite}$	$(2.7-3) \times 10^{-4}$	250	120	10	$\text{Mn}_3\text{O}_4, 29.2, \text{CuO}, 21.6, \text{NiO}, 10.7; \Sigma = 61.5$
No. 3, extrudates, $d = 0.25$ cm, based on $\text{MnCO}_3$ , supplied from Russia	$\text{Mn}_2\text{O}_4, \text{CaCO}_3, \text{NiO}, \text{CuO}, \text{CA}_2$	$2.2 \times 10^{-4}$	260	120	60	$\text{Mn}_3\text{O}_4, 30.2, \text{CuO}, 20.4, \text{NiO}, 11.3; \Sigma = 61.9$
No. 4, extrudates, $d = 0.30$ cm, based on $\text{MnCO}_3$ , supplied from Russia	$\text{Mn}_3\text{O}_4, \text{CaCO}_3, \text{CA}_2, \text{MnCO}_3, \text{NiO}, \text{CuO}$	$(2.1-2.2) \times 10^{-4}$	260	90	60	$\text{Mn}_3\text{O}_4, 28.0, \text{CuO}, 22.7, \text{NiO}, 10.4; \Sigma = 61.1$
No. 5, molded pellets, $d \times h = 5 \times 3$ mm, November 2004, based on $\text{MnCO}_3$ , supplied from Belgium	$\text{CuO}, \text{MnO}_2, \text{Mn}_3\text{O}_4, \text{trace amounts CA}_2, \text{NiO}, \text{CaCO}_3, \text{aragonite}, \text{MnCO}_3$	$1.58 \times 10^{-4}$	220	110	40	$\text{Mn}_3\text{O}_4, 30.3, \text{CuO}, 20.2, \text{NiO}, 9.0; \Sigma = 59.5$
No. 6, molded pellets, $d \times h = 5 \times 3$ mm, June 2005, based on $\text{MnCO}_3$ , supplied from Belgium	$\text{CuO}, \text{MnO}_2, \text{MnCO}_3, \text{Mn}_3\text{O}_4, \text{CA}_2, \text{CA}, \text{NiO}, \text{CaCO}_3, \text{trace amounts}$	$1.90 \times 10^{-4}$	220	100	60	$\text{Mn}_3\text{O}_4, 26.5, \text{CuO}, 20.5, \text{NiO}, 9.5; \Sigma = 56.5$
No. 7, molded pellets, $d \times h = 5 \times 3$ mm, June 2005, based on $\text{MnCO}_3$ , supplied from Bulgaria	$\text{CuO}, \text{Mn}_3\text{O}_4, \text{MnO}_2, \text{MnCO}_3, \text{CA}_2, \text{CaCO}_3, \text{NiO}, \text{aragonite}, \text{trace amounts}, \text{CA}$	$2.35 \times 10^{-4}$	230	110	70	$\text{Mn}_3\text{O}_4, 27.1, \text{CuO}, 20.5, \text{NiO}, 9.0; \Sigma = 56.6$

ponent (Table 5), which can also account for the decrease in  $\gamma$ . The catalytic activities of these batches in benzene oxidation do not differ significantly.

Molded pellets were produced on industrial equipment (FP-025 pellet-granulator, manufactured by Dzerzhinsk NIIkhimmash federal state unitary enterprise) from manganese carbonate from Belgium, which contains an insignificant amount of  $\text{Mn}_2\text{O}_3$  (GTT catalyst batch nos. 5 and 6), and manganese carbonate manufactured in Bulgaria, which contains no  $\text{Mn}_2\text{O}_3$  (catalyst batch no. 7) (Table 5). It was found that the ozone decomposition factor  $\gamma$  for GTT no. 7 is, on average, 1.4 times that for GTT nos. 5 and 6. It is, however, impossible to state unambiguously that the brand of  $\text{MnCO}_3$  affects the catalytic activity

of GTT in ozone decomposition in the case of industrial batches. It can be seen from the data presented that there is difference in porosities (by a factor of 1.17–1.5) even for batches prepared from the same brand of raw material, manganese carbonate manufactured in Belgium. The catalytic activities of these batches in benzene oxidation do not differ significantly.

A comparison of the basic characteristics of GTT batches produced under pilot-industrial conditions (extrudates of various diameters) and manufactured under industrial conditions (molded pellets) at the same calcination temperature demonstrated that that the activity of extrudates in ozone decomposition exceeds that of molded pellets by, on average, a factor

of 1.1–1.7 and that in benzene oxidation is lower (benzene oxidation temperature at 50% conversion is, on average, 30–40°C higher) (Table 5). These batches show insignificant differences in porosity, specific surface area, and amount of the active component. It can be assumed that the changes in activity are due to specific features of the decomposition of the starting manganese carbonates in the extrudates and pellets in the calcination stage. It has been found previously that the type of a manganese-containing phase formed is sensitive to the calcination temperature. In the range  $T = 300\text{--}350^\circ\text{C}$ , the  $\text{MnO}_2$  phase is formed in extrudates (Table 3), with the benzene oxidation temperature at 50% conversion equal to  $230^\circ\text{C}$  (Fig. 1) and  $\gamma = (2.22\text{--}2.38) \times 10^{-4}$ . In the range  $T = 400\text{--}450^\circ\text{C}$ ,  $\text{Mn}_3\text{O}_4$  is the main manganese-containing phase, with  $T_{\text{benz.ox}} = 240\text{--}280^\circ\text{C}$  and  $\gamma = 2.45 \times 10^{-4}$ . In molded pellets, the  $\text{MnO}_2$  phase is still present at  $T = 400\text{--}430^\circ\text{C}$ , the benzene oxidation temperature at 50% conversion is  $220\text{--}230^\circ\text{C}$ , and  $\gamma = (1.58\text{--}2.35) \times 10^{-4}$  (Table 5). Presumably, the predominance of the manganese-containing phase  $\text{Mn}_3\text{O}_4$  in GTT samples (extrudates, pellets) at calcination temperatures in the range  $300\text{--}450^\circ\text{C}$  favors an increase in the activity of the catalyst in ozone decomposition, and the presence of the  $\text{MnO}_2$  phase positively affects the activity in benzene oxidation.

According to the quality regulations for manganese-containing raw materials, the mass fraction of sulfur in terms of sulfates should not exceed 0.04%. The content of sulfur in the manganese-containing starting component, especially of domestic or Bulgarian manufacture, fails to satisfy these requirements. A number of test batches were prepared in the form of extrudates based on manganese carbonates containing 0.16 to 0.23% sulfates ( $\text{SO}_4^{2-}$ ). In the finished catalyst, the content of sulfates varied from 0.08 to 0.11%. In this case, the ozone decomposition factor was  $\gamma = (2.1\text{--}2.7) \times 10^{-4}$ , which points to a high activity of the catalyst. Also, the benzene oxidation temperature at 50% conversion was found to be  $240\text{--}260^\circ\text{C}$  for this catalyst.

When preparing molded pellets, manganese carbonates containing 0.0076–0.026, 0.56–0.69, and 0.77–1.14% sulfates were used. The mass fractions of  $\text{SO}_4^{2-}$  in the finished catalysts were 0.0065–0.025, 0.032–0.15, and 0.197–0.36%, respectively. In this case, the ozone decomposition factors are  $(1.35\text{--}1.85) \times 10^{-4}$ ,  $(1.85\text{--}2.4) \times 10^{-4}$ , and  $(2.0\text{--}2.4) \times 10^{-4}$ , respectively, which corresponds to a high catalytic activity in ozone decomposition. The catalytic activities of these batches in benzene oxidation were evaluated by the benzene oxidation temperature at 50% conver-

sion:  $210\text{--}230$ ,  $220\text{--}230$ , and  $220\text{--}230^\circ\text{C}$ , respectively.

Laboratory samples were produced with manganese carbonates containing 0.008 and 0.7% sulfates. The mass fraction of sulfates in the finished catalyst was 0.004 and 0.12%, respectively. The samples exhibited virtually the same activity in ozone decomposition:  $\gamma = (1.9 \pm 0.2) \times 10^{-4}$ . The benzene oxidation temperature at 50% conversion was  $220$  and  $240^\circ\text{C}$ .

It can be seen from these data that the mass fraction of sulfur in terms of sulfides in the starting manganese-containing component has no effect on the catalytic activity of the GTT catalyst in both ozone decomposition and benzene oxidation. It is known that a requirement to the purity of starting components affects their cost. Consequently, less expensive raw materials can be used in GTT manufacture. Industrial batches of the catalysts developed have been manufactured to order of TIMIS Research-and-Promotion Firm, Limited Liability Company at Novomoskovsk Institute of nitrogen industries and successfully work in ozonizer installations at more than 40 plants of Russia, Ukraine, Thailand, and Switzerland [14–16].

GTT catalysts are also effectively used in gas-convectors of the gas-discharge type, intended for purification of ventilation gases and recycled and influent air to remove toxic substances, such as butanol, styrene, toluene, phenol, benzene, formaldehyde, aniline, etc., formed in operation of motor transport, technological equipment, and public feeding facilities. Air is purified in a gas-convector under the action of an electric discharge on molecule of gases present in the discharge zone.

## CONCLUSIONS

(1) An integrated study of the process in which catalysts for ozone decomposition are formed from copper and nickel hydroxocarbonates, manganese carbonate, and calcium aluminates (talam) demonstrated that a heterogeneous ion exchange occurs between the components in the course of preparation, to give precursors of the active phase.

(2) It was shown that presence of the manganese-containing phase  $\text{Mn}_3\text{O}_4$  in GTT samples (extrudates, pellets) favors, at calcination temperatures of  $300\text{--}450^\circ\text{C}$ , an increase in the catalytic activity in ozone decomposition, and presence of the  $\text{MnO}_2$  phase positively affects the activity in benzene oxidation. The optimal GTT calcination temperatures for ozone decomposition and benzene oxidation were determined.

(3) It was demonstrated that the catalytic activity of the GTT catalyst in both ozone decomposition and benzene oxidation is not affected to any significant extent by the composition of the manganese-containing raw material and by the amount of sulfur (in the concentration range studied) in the starting components.

(4) Extrudates with a diameter of 1.5–5 mm and length of 5–15 mm and molded pellets [ $d \times h = 5 \times 3$  ( $4 \times 3$ ) mm<sup>2</sup>] were produced. The catalyst obtained exhibits high activity and mechanical strength in operation in both dry and humid gases.

#### REFERENCES

1. Rodionov, A.I., Klushin, V.N., and Torocheshnikov, N.S., *Tekhnika zashchity okruzhayushchei sredy* (Environment Protection Technology), Moscow: Khimiya, 1989.
2. Tkachenko, S.N., Homogeneous and Heterogeneous Decomposition of Ozone, *Doctoral Dissertation*, Moscow, 2004.
3. Tkachenko, S.N., Golosman, E.Z., and Lunin, V.V., *Kataliz Prom-sti*, 2001, no. 2, p. 52.
4. Lunin, V.V., Popovich, M.P., and Tkachenko, S.N., *Fizicheskaya khimiya ozona* (Physical Chemistry of Ozone), Moscow: Mosk. Gos. Univ., 1998.
5. RF Patent 2077946.
6. USSR Inventor's Certificate, no. 1768274.
7. Makhov, E.A., Tkachenko, S.N., Golosman, E.Z., et al., *Khim. Prom-st. Segodnya*, 2003, no. 7, p. 11.
8. Yakerson, V.I. and Golosman, E.Z., *Katalizatory i tsementy* (Catalysts and Cements), Moscow: Khimiya, 1992.
9. Tkachenko, S.N., Lunin, V.V., Egorova, G.V., et al., *The Int. Ozone Association: 17th world congress* (IOA 17), Ozone and Related Oxidants, Innovative and Current Technologies, Strasbourg, France, August 22–25, 2005, p. 50.
10. Golosman, E.Z., *Kinet. Kataliz*, 2001, vol. 42, no. 3, pp. 383–393.
11. Golosman, E.Z. and Yakerson, V.I., *Proizvodstvo i ekspluatatsiya promyshlennykh tsementsoderzhashchikh katalizatorov* (Manufacture and Use of Industrial Cement-containing Catalysts), Available from NIITEKhim, 1992, Cherkassy, no. 287-khp-92.
12. Nechugovskii, A.I., Grechenko, A.N., and Golosman, E.Z., *Zh. Prikl. Khim.*, 1990, vol. 63, no. 8, pp. 1747–1751.
13. Troshina, V.A., Mamaeva, I.A., Salomatin, G.I., et al., *Zh. Prikl. Khim.*, 2003, vol. 76, no. 3, pp. 430–436.
14. RF Patent 2163836.
15. Demidyuk, V.I., Tkachenko, S.N., Makhov, E.A., et al., *Kataliz Prom-sti*, 2003, no. 6, pp. 42–46.
16. Tkachenko, S.N., Demidyuk, V.I., Egorova, G.V., et al., *Khim. Prom-st.*, 1992, no. 10, p. 604.